



## First observation of micrometeoroid differential ablation in the atmosphere

D. Janches,<sup>1</sup> L. P. Dyrud,<sup>2</sup> S. L. Broadley,<sup>3</sup> and J. M. C. Plane<sup>3</sup>

Received 20 January 2009; accepted 18 February 2009; published 20 March 2009.

[1] Every day, billions of microgram-sized-extraterrestrial particles enter and ablate in the upper layers of the Earth's atmosphere, depositing their mass in the mesosphere and lower thermosphere (MLT). This evaporated meteoric mass is the source of global layers of neutral metal atoms, sporadic E layers of metal ions, and meteoric smoke particles. Because their kinetic energy is insufficient to produce detectable optical emissions, these particles can only be observed using sensitive radars, which detect the plasma (i.e., electrons) either immediately surrounding the meteoroid (head-echo), or left behind along its path (trail-echo). Here we show that observed short-scale temporal features in the radar returned signal from the meteor head-echo are explained by differential ablation of the chemical constituents. These results represent the first observation of this mass-loss process, indicating that this is the main mechanism through which the meteoric mass of micron-sized particles is deposited in the MLT. **Citation:** Janches, D., L. P. Dyrud, S. L. Broadley, and J. M. C. Plane (2009), First observation of micrometeoroid differential ablation in the atmosphere, *Geophys. Res. Lett.*, 36, L06101, doi:10.1029/2009GL037389.

### 1. Introduction

[2] Sporadic meteoroids in the mass range of  $10^{-11}$  to  $10^{-4}$  g entering the Earth's atmosphere at very high entry velocities undergo rapid frictional heating by collision with air molecules, and their constituent minerals subsequently vaporize. This provides the dominant source of various metals and silicon in the mesosphere and lower thermosphere (MLT) [Williams and Murad, 2002], which are manifest as layers of neutral metal atoms (Na, Fe, Ca etc.), sporadic E layers, and meteoric smoke particles [e.g., Hunten et al., 1980; Kalashnikova et al., 2000; Plane, 2003; Saunders and Plane, 2006].

[3] Because these particles are small, they do not have sufficient kinetic energy upon atmospheric entry to produce significant amount of light to be observed by common meteor cameras and they are mostly detected through the manifestation of radar echoes. Since radars detect only electrons, it is challenging to understand in detail the ablation processes through which these are produced while the micrometeoroid chemical constituents are deposited in

the MLT. The production of electrons depends on the ionization probability of the evaporating constituents,  $\beta$  [Jones, 1997; Jones and Halliday, 2001], which depends both on meteoroid velocity and each chemical element. Radar detectability of meteors has usually been estimated by using a crude average of this parameter, weighted by the relative abundances of the major constituents [Close et al., 2002]. However, this hides the very different dependencies of  $\beta$  on meteoroid velocity for each chemical constituent.

[4] Recently, Vondrak et al. [2008] developed a model of the micrometeoroid differential ablation that considers for the first time the full treatment of the ablation and ionization of the individual chemical elements and showed that  $\beta$  can vary up to 2 orders of magnitude depending on the constituent being considered.

[5] Through the differential ablation process, the particle's more volatile elements (Na and K) are released first when its temperature is still relatively low. As the meteoroid penetrates deeper into the atmosphere and the atmospheric density increases, the particle collides with a sufficient number of air molecules to raise its temperature to the point ( $\sim 1800$  K) where the main chemical constituents (Si, Fe and Mg) evaporate. This will occur  $\sim 12$  km lower than where the alkalis were evaporated first. Finally, the ablation of the most refractory meteoroid constituents (mostly Ca, Ti and Al) will occur only if the particle's kinetic energy is sufficient to raise its temperature beyond  $\sim 2500$  K [Vondrak et al., 2008]. This differential ablation model, which is based on fractionation models used by planetary scientists [Fegley and Cameron, 1987], was first proposed by McNeil et al. [1998] to explain the large depletion of Ca to Na observed in meteor trails [von Zahn et al., 1999].

[6] In this work, we present the first observations of differential ablation in micrometeoroids, using head-echo events detected with the 430 MHz Arecibo radar in Puerto Rico [Janches et al., 2003]. In the past, spectroscopy measurements in normal bright meteors [Borovička et al., 2007] have shown that different elements ablate at different points along the train. However, these are relatively large particles (not micrometeoroids) which are comparatively rare and hence do not constitute the bulk of the incoming material [Williams and Murad, 2002]. In the case of large meteoroids (mass  $> 5$  mg), the isothermal condition during atmospheric entry does not hold [Vondrak et al., 2008], and so the results of fireball spectroscopy are not directly comparable with the smaller particles under consideration here.

### 2. Model Description

[7] We utilize two state-of-the-art models to correlate temporal behavior in the received signal of observed radar meteor head-echoes with the precise moment and altitude at

<sup>1</sup>Colorado Research Associates, NorthWest Research Associates, Boulder, Colorado, USA.

<sup>2</sup>Center for Remote Sensing, Inc., Fairfax, Virginia, USA.

<sup>3</sup>School of Chemistry, University of Leeds, Leeds, UK.

which a particular chemical constituent is predicted to evaporate from the main body. The first model is a new meteoric Chemical Ablation Model (CAMOD) [Vondrak *et al.*, 2008], which treats the physics and chemistry of ablation by including the following processes: sputtering by inelastic collisions with air molecules before the meteoroids melt; evaporation of atoms and oxides from the molten particle; diffusion-controlled migration of the volatile constituents (Na and K) through the molten particle; and impact ionization of the ablated fragments by hyperthermal collisions with the air molecules. Evaporation is based on thermodynamic equilibrium in the molten meteoroid (treated as a melt of metal oxides), and between the particle and surrounding vapour phase. The loss rate of each element is then estimated by applying Langmuir evaporation. The initial composition of the meteoroids is assumed to be chondritic [Plane, 1991]. The major constituents by elemental abundances are then: O 56.3%, Mg 14.4%, Si 13.6%, Fe 12.1%, Al 1.2%, Ca 0.82%, Na 0.80% and K 0.05% [Vondrak *et al.*, 2008].

[8] The second model is based upon a parameterization of hundreds of Finite Difference Time Domain (FDTD) simulations of electromagnetic waves interacting with the meteor plasma to estimate the meteor Radar Cross Section (RCS) [Dyrud *et al.*, 2007a, 2007b]. The shape and density of the meteor head-echo plasma is estimated from the electron line density and meteor velocity as a function of altitude modelled by CAMOD. Once the RCS is estimated, a parameterization of the Arecibo radar beam is used to obtain the detected meteor SNR [Dyrud and Janches, 2008].

[9] The innovative aspect of the present study is that, for the first time, we estimate meteor RCS and SNR considering  $\beta$  separately for each constituent. This allows us to trace the detectability of each element along the observed path of the meteoroid, and hence reproduce very short time scale features of the recorded meteor SNR, which were previously unexplained.

### 3. Methodology and Results

[10] Figures 1 and 2 illustrate the application of the models to two distinctly different examples observed on January 22, 2002 (referred to hereafter as Cases 1 and 2, respectively). These events are examples of the thousands of meteor events observed daily by the Arecibo 430 MHz radar, and although in this paper we present just two cases, this methodology has been successfully applied on a routine basis to a broad range of velocities and masses. Dyrud and Janches [2008] presented the same SNR and Doppler fitting technique, but used the more standard ablation equations, and found that those ablation profiles could not account for the occasional SNR curves that were non-smooth, such as those presented here. In Figures 1a and 2a, the Range-Time-Intensity (RTI) image of the meteor is displayed. The vertical spread of the meteor is due to the square shape of the transmitted pulse [Janches *et al.*, 2003]. The white dash-dot line shows the leading edge of the pulse from where the meteor altitude as a function of time is measured [Janches and ReVelle, 2005]. For Case 1, the initial observed altitude is 110 km and final is 103 km. For Case 2, the meteor is first observed at an altitude of 103.5 km, disappearing from the

radar beam when it reached 96 km. The measured instantaneous meteor velocity along the line of sight (LOS) (vertical in this case [Janches *et al.*, 2003]) is displayed in diamonds in Figures 1b and 2b. The measured LOS velocity for Case 1 is  $35 \text{ km s}^{-1}$ , and no strong deceleration occurs. For Case 2, in contrast, the LOS velocity is initially  $50 \text{ km s}^{-1}$ , slowing down by  $5 \text{ km s}^{-1}$  during the time it was observed. The measured head-echo SNR is displayed as a thick red line in Figures 1c and 2c; in both cases sudden changes in the measured SNR were observed. For Case 1, Figures 1a and 1c show that there was a sudden enhancement of the measured meteor SNR at 106.5 km over an altitude range of 1 km. For Case 2, a sudden sharp decrease of signal strength occurred at 99.5 km, 60 msec after the event was first detected.

[11] The calculated errors in the velocity are of the order of  $\text{m s}^{-1}$  when SNR is high [Janches *et al.*, 2003], and become large, as seen at the edges of observations, when SNR is low. The fact that the velocity estimates follow a smooth evolution in altitude and time, before and after the changes in SNR occurred, indicates that the meteoroid did not undergo an abrupt physical modification (such as fragmentation [Kero *et al.*, 2005; Mathews *et al.*, 2007]). The smooth increase of meteor SNR before these features is easily explained by considering the increase in electron production from a particle which is interacting with more and more air molecules, together with the fact that the particle is entering the higher transmitted power density region of the radar beam [Dyrud and Janches, 2008]. Thus, the abrupt changes in SNR must be related to a sudden increase (Case 1) or decrease (Case 2) in the rate of production of electrons giving rise to the meteor head plasma.

[12] To study these effects, we utilize the two models described earlier, iterating meteoroid parameters as well as using a least-squares fitting routine [Dyrud and Janches, 2008] until we obtain agreement between the CAMOD predictions coupled with the plasma model and the measured SNR and velocity profiles as shown in Figures 1b, 2b, 1c, and 2c (thin black lines). We begin by coarsely iterating three input parameters for CAMOD: the particle entry angle, mass and density (the vertical component of the particle velocity is constrained by the measured line-of-sight velocity at the start of the event). The resulting height profiles of the electron production rate are then used as input to the plasma model. In order to obtain sensible agreement with the radar observations, we used this second model to fit for distance from the radar beam center of the meteoroid trajectory, altitude where the trajectory makes closest approach to beam center, and a final and finer fit to the zenith angle allowing it to vary by  $\pm 3$  degrees from the initial ablation zenith angle. The resulting best fit parameters for Case 1 are: initial velocity =  $36 \text{ km s}^{-1}$ ; entry angle =  $1^\circ$  (to zenith); mass =  $10^{-8} \text{ kg}$ ; density =  $3500 \text{ kg m}^{-3}$ . For Case 2: velocity =  $51 \text{ km s}^{-1}$ ; entry angle =  $10^\circ$ ; mass =  $10^{-8} \text{ kg}$ ; density =  $2500 \text{ kg m}^{-3}$ . The best-fit to the meteor LOS velocity and SNR resulting from the ablation and ionization predictions from CAMOD are displayed in Figures 1d, 2d, 1e, and 2e. For Case 1, Figure 1e shows that the enhancement in meteor SNR is produced by the rapid and complete evaporation of Na and K, well before the ablation of the major constituents is significant. The esti-

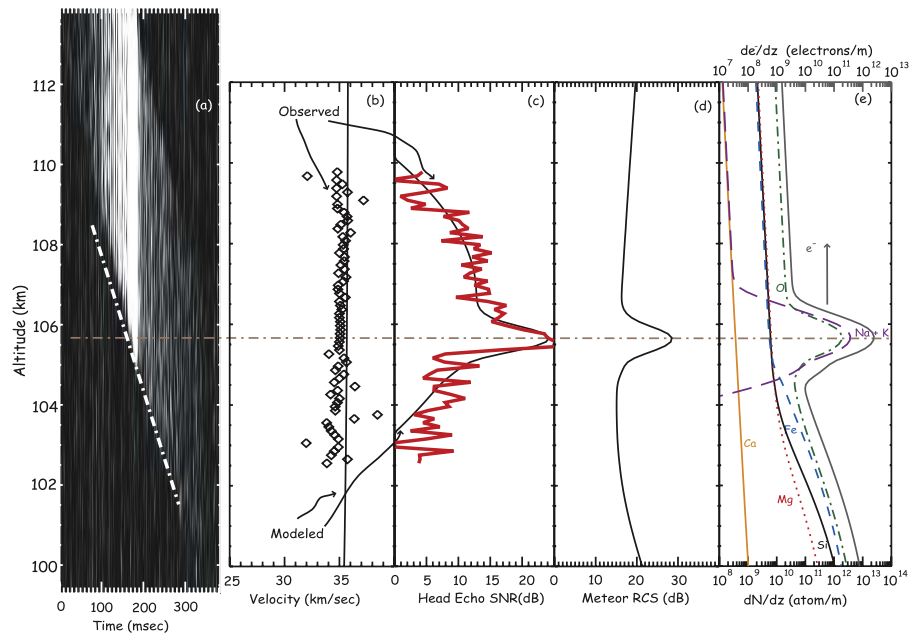


**Figure 1.** Observed and modelled “slow” meteor event (Case 1). (a) Meteor RTI. (b) Modelled (line) and observed (diamonds) meteor altitude-velocity profile. (c) Modelled (black) and observed (red) meteor SNR. (d) Modelled meteor RCS. (e) Ablation profiles of main elements (bottom axis) and total amount of electrons produced (upper axis). The horizontal line across the plots shows that the observed enhancement in SNR is due to the rapid ablation of the alkali metals Na and K.

mated RCS, which is derived from the electron production rate predicted by CAMOD (grey line in Figure 1e), is displayed in Figure 1d. The resulting modelled enhancement in the head echo agrees very well with the observation, as shown in Figure 1c.

[13] For Case 2, the scenario is somewhat different. This meteor was much faster, and was detected significantly lower than the first example. It is clear from the model that the sharp decrease in the production of electrons, and thus of the meteor SNR, was due to the complete ablation of the

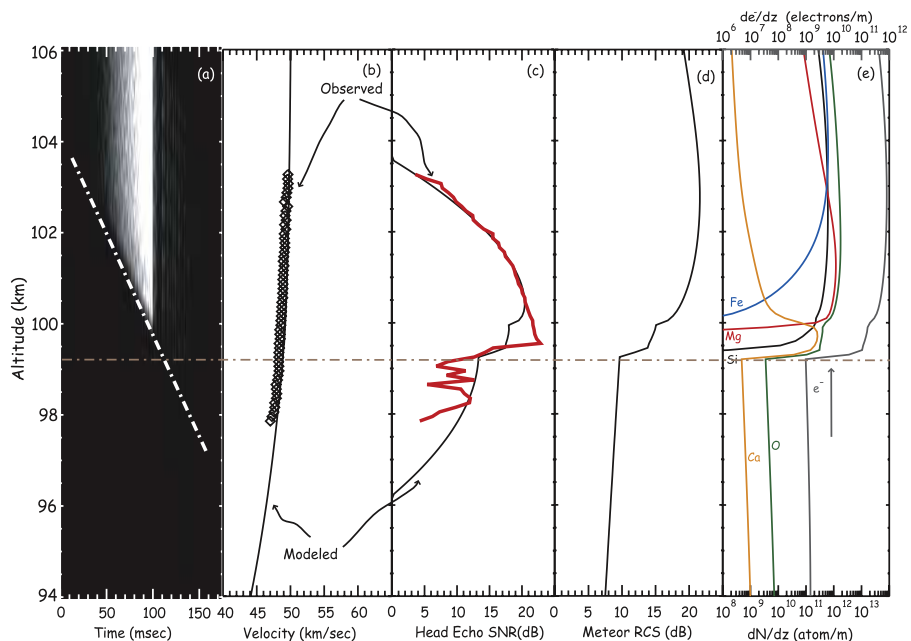


**Figure 2.** A “fast” meteor event (Case 2, same format as Figure 1). The horizontal (dash-dot) line across the plots marks the observed sudden decrease in SNR, which coincides with the complete ablation of the main constituents (Si, Fe and Mg). The particle remained visible after the relatively volatile elements evaporated because it then heated rapidly to almost 5000 K and the most refractory elements (Ca, Al and Ti) completely evaporated.

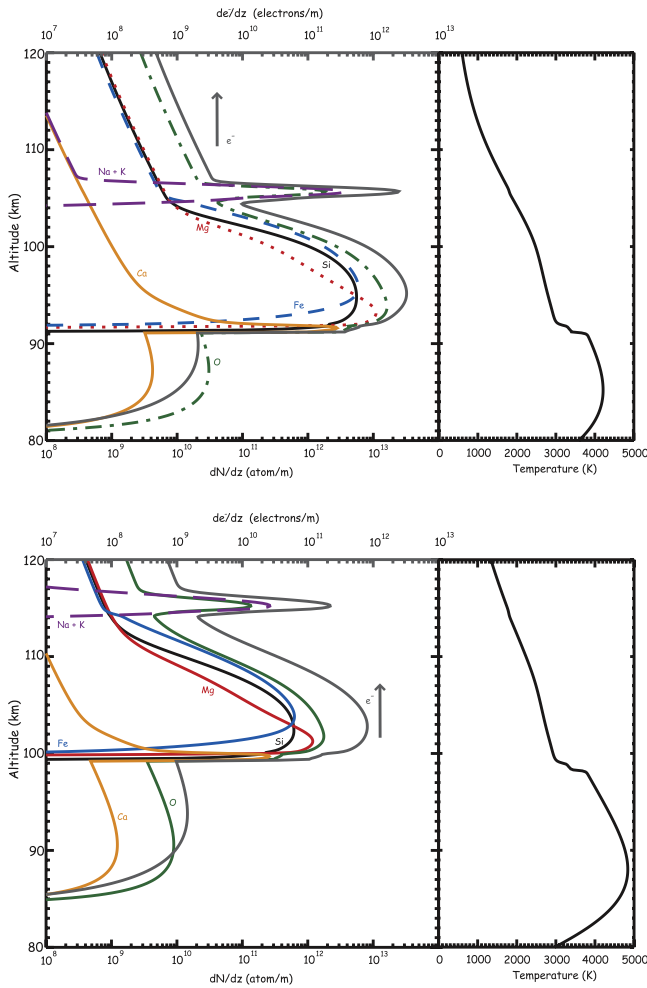


**Figure 3.** Ablation profiles of the individual elements and the meteoroid temperature, for (top) Case 1 and (bottom) Case 2.

main meteoroid constituents (Si, Fe and Mg). The much reduced SNR below 100 km is caused by the ablation of the refractory metals (Ca is shown, Al and Ti are also significant).

#### 4. Discussion

[14] To place in context the results of Figures 1 and 2, we show in Figure 3 the entire elemental deposition profiles together with the estimated meteoroid temperature for both cases. For the slower meteoroid (Case 1), Na and K are released at 106 km, while for the faster case the evaporation of these constituents occurs much higher (114 km) due to its higher kinetic energy. In both cases, their vaporization is almost complete before other elements start to evaporate. For Case 1, this is the moment at which the meteoroid traveled through the radar beam, thus allowing the detection of the SNR enhancement. The meteoroid left the radar beam soon after the alkalis had evaporated. If this meteoroid had intersected the radar beam at a lower altitude, the SNR altitude profile would have exhibited a smooth curve

resulting from the more prolonged ablation of the main meteoroid constituents. This is in fact what occurs in the majority of detected events [Dyrud and Janches, 2008].

[15] Figure 3 shows that the peak release of the less volatile constituents Si, Fe and Mg occurs 10–15 km lower in the atmosphere. For Case 2, the ablation of Na and K occurred before the meteoroid entered the radar beam, which explains why no enhancement was observed. The meteoroid was detected initially during the ablation of the main constituents. At this point the mass loss rate is sufficient to limit the temperature rise of the particle. Once the Si, Fe and Mg have evaporated and the residual particle is essentially refractory CaO, AlO and TiO, the rate of evaporation and hence electron production collapses, causing the sudden drop in the RCS at 99.5 km. However, without significant mass loss to balance the frictional heating of the particle, its temperature increases rapidly to almost 5000 K (Figure 3, bottom) and the refractory elements evaporate. We are not aware of direct observations of these high temperatures predicted by the model. Fireball spectroscopy indicates that the temperature of the gas surrounding a relatively large meteoroid reaches a temperature of  $\sim 4300$  K [Borovicka, 1994], but this is not the temperature of the molten particle itself. This does not occur for the slower particle (Case 1), where the slower and smoother evaporation of the major constituents below 100 km was sufficient to make the meteor observable at a lower SNR (Figure 1a).

[16] Finally, it is important to note that the observable features of the differential ablation process appear only in a small percentage of thousands of radar echoes detected daily. This is mainly due to two reasons: 1) the relatively short duration of the feature with respect to the entire echo light curve decreases the chances of occurrence inside the very narrow Arecibo radar beam ( $\sim 300$  m in diameter); and 2) the features become less discernable for various combinations of meteoroid velocity and mass. Future work will concentrate on a statistical study of these features.

#### 5. Conclusions

[17] We presented in this paper the first observation of meteoroid differential ablation. Our results suggest that this is the main mechanism through which micron-sized particles deposit their mass in the Mesosphere and Lower Thermosphere. These results are obtained utilizing two state-of-the-art models to correlate temporal behavior in the received signal of observed radar meteor head-echoes with the precise moment at which a particular chemical constituent is predicted to evaporate from the main body. This is possible because we treat  $\beta$  separately for each constituent instead of using a crude average as done in previous works, allowing us to correlate very different features with the same physical and chemical process. The coupling of a differential ablation model such as CAMOD with an astronomical model of the meteoric flux [Fentzke and Janches, 2008] combined with large aperture radar observations, will therefore enable the origins of meteoroids within the solar system to be related to the deposition of their constituents in the upper atmosphere, and shed new light on their aeronomical impacts.

[18] **Acknowledgments.** The Arecibo Observatory is part of the National Astronomy and Ionosphere Center, which is operated by Cornell University under cooperative agreement with the National Science Foundation. Also, the authors wish to thank Naomi Edelberg for her help on the analysis of the AO meteor data. DJ was supported under NSF grants ATM-05311464 and ATM-0525655 to NorthWest Research Associates, Inc and agreement 51861-8406 between Cornell University and Nwra. LPD was supported under NSF grants ATM-0613706 and ATM-0638912. JMCP and SB were supported under NERC grant NE/B00015X/1. The authors thank T. Vondrak for assistance in running the CAMOD ablation model.

## References

- Borovička, J. (1994), Two components in meteor spectra, *Planet. Space Sci.*, *42*, 145–150, doi:10.1016/0032-0633(94)90025-6.
- Borovička, J., P. Spurný, and P. Koten (2007), Atmospheric deceleration and light curves of Draconid meteors and implications for the structure of cometary dust, *Astron. Astrophys.*, *473*, 661–672, doi:10.1051/0004-6361:20078131.
- Close, S., M. Oppenheim, S. Hunt, and L. Dyrud (2002), Scattering characteristics of high-resolution meteor head echoes detected at multiple frequencies, *J. Geophys. Res.*, *107*(A10), 1295, doi:10.1029/2002JA009253.
- Dyrud, L. P., and D. Janches (2008), Modeling the meteor head-echo using Arecibo radar observations, *J. Atmos. Sol. Terr. Phys.*, *70*, 1621–1632, doi:10.1016/j.jastp.2008.06.016.
- Dyrud, L., D. Wilson, S. Boerve, J. Trulsen, H. Pecseli, S. Close, C. Chen, and Y. Lee (2007a), Plasma and electromagnetic simulations of meteor head echo radar reflections, *Earth Moon Planets*, *102*, 383–394, doi:10.1007/s11038-007-9189-8.
- Dyrud, L., D. Wilson, S. Boerve, J. Trulsen, H. Pecseli, S. Close, C. Chen, and Y. Lee (2007b), Plasma and electromagnetic wave simulations of meteors, *Adv. Space Res.*, *42*, 136–142, doi:10.1016/j.asr.2007.03.048.
- Fegley, B., and A. G. W. Cameron (1987), A vaporization model for iron/silicate fractionation in the Mercury protoplanet, *Earth Planet. Sci. Lett.*, *82*, 207–222, doi:10.1016/0012-821X(87)90196-8.
- Fentzke, J. T., and D. Janches (2008), A semi-empirical model of the contribution from sporadic meteoroid sources on the meteor input function in the MLT observed at Arecibo, *J. Geophys. Res.*, *113*, A03304, doi:10.1029/2007JA012531.
- Hunten, D. M., R. P. Turco, and O. B. Toon (1980), Smoke and dust particles of meteoric origin in the mesosphere and stratosphere, *J. Atmos. Sci.*, *37*, 1342–1357.
- Janches, D., and D. O. ReVelle (2005), Initial altitude of the micrometeoroid phenomenon: Comparison between Arecibo radar observations and theory, *J. Geophys. Res.*, *110*, A08307, doi:10.1029/2005JA011022.
- Janches, D., M. C. Nolan, D. D. Meisel, J. D. Mathews, Q. H. Zhou, and D. E. Moser (2003), On the geocentric micrometeoroid velocity distribution, *J. Geophys. Res.*, *108*(A6), 1222, doi:10.1029/2002JA009789.
- Jones, W. (1997), Theoretical and observational determinations of the ionization coefficient of meteors, *Mon. Not. R. Astron. Soc.*, *288*, 995–1003.
- Jones, W., and I. Halliday (2001), Effects of excitation and ionization in meteor trains, *Mon. Not. R. Astron. Soc.*, *320*, 417–423, doi:10.1046/j.1365-8711.2001.03833.x.
- Kalashnikova, O., M. Horányi, G. E. Thomas, and O. B. Toon (2000), Meteoric Smoke Production in the Atmosphere, *Geophys. Res. Lett.*, *27*, 3293–3296, doi:10.1029/1999GL011338.
- Kero, J., C. Szasz, A. Pellinen-Wannberg, G. Wannberg, and A. Westman (2005), Power fluctuations in meteor head echoes observed with the EISCAT VHF radar, *Earth Moon Planets*, *95*, 633–638, doi:10.1007/s11038-005-3090-0.
- Mathews, J. D., S. J. Briczinski, D. D. Meisel, and C. J. Heinselman (2007), Radio and Meteor Science Outcomes From Comparisons of Meteor Radar Observations at AMISR Poker Flat, Sondrestrom, and Arecibo, *Earth Moon Planets*, *102*, 365–372, doi:10.1007/s11038-007-9168-0.
- McNeil, W., S. Lai, and E. Murad (1998), Differential ablation of cosmic dust and implications for the relative abundances of atmospheric metals, *J. Geophys. Res.*, *103*, 10,899–10,911.
- Plane, J. M. C. (1991), The chemistry of meteoric metals in the upper atmosphere, *Int. Rev. Phys. Chem.*, *10*, 55–106.
- Plane, J. M. C. (2003), Atmospheric chemistry of meteoric metals, *Chem. Rev.*, *103*, 4963–4984.
- Saunders, R. W., and J. M. C. Plane (2006), A laboratory study of meteor smoke analogues: Composition, optical properties and growth kinetics, *J. Atmos. Sol. Terr. Phys.*, *68*, 2182–2202, doi:10.1016/j.jastp.2006.09.006.
- Vondrak, T., S. L. Broadley, J. M. C. Plane, and D. Janches (2008), A new chemical model of meteoroid ablation, *Atmos. Chem. Phys. Discuss.*, *8*, 14,557–14,606.
- von Zahn, U., M. Gerding, J. Höffner, W. J. McNeil, and E. Murad (1999), Iron, calcium, and potassium atom densities in the trails of Leonids and other meteors: Strong evidence for differential ablation, *Meteorit. Planet. Sci.*, *34*, 1017–1027.
- Williams, I. P., and E. Murad (2002), Introduction, in *Meteors in the Earth's Atmosphere*, edited by E. Murad and I. P. Williams, pp. 1–10, Cambridge Univ. Press, Cambridge, U. K.

S. Broadley and J. M. C. Plane, School of Chemistry, University of Leeds, Woodhouse Lane, Leeds LS2 9JT, UK. (chmslb@leeds.ac.uk; j.m.c.plane@leeds.ac.uk)

L. P. Dyrud, Center for Remote Sensing, Inc., 3702 Pender Drive, Fairfax, VA 22030, USA. (ldyrud@cfrsi.com)

D. Janches, Colorado Research Associates, NorthWest Research Associates, 3380 Mitchell Lane, Boulder, CO 80301, USA. (diego@cora.nwra.com)